Yield and recoil properties of iodine isotopes from the interaction of 240 MeV ^{12}C with ^{238}U

Y. W. Yu and C. H. Lee
College of Nuclear Science, National Tsing-Hua University, Taiwan, Republic of China

K. J. Moody,* H. Kudo,† D. Lee, and G. T. Seaborg
Nuclear Science Division, Lawrence Berkeley Laboratory, University of California, Berkeley, California 94720
(Received 9 March 1987)

The independent yields, recoil properties, and forward-to-backward ratios (F/B) of iodine isotopes from the interaction of 240 MeV ^{12}C with ^{238}U have been measured radiochemically by the thick-target/thick-catcher method. The isotopic yield distribution curve has been constructed and is found to consist of two overlapping Gaussians, peaking at $A=126.5$ and 133.8 with width parameters of 2.29 and 2.04 mass units, respectively. All the measured iodine isotopes had ranges of 7.7 ± 0.4 mg/cm^2. The neutron-deficient products have F/B of 1.76 ± 0.14, but the neutron-excessive products have F/B of only 1.09 ± 0.06. The yield curve was analyzed with the liquid drop model and the recoil curve was analyzed by the standard two-step vector model; the results show that the neutron-deficient products are formed from nonequilibrium processes and the neutron-excessive products are formed from the normal low-energy fission process.

I. INTRODUCTION

In recent years heavy-ion reactions have been studied intensively. A large amount of data on the interaction of ^{12}C with ^{238}U have been reported with high energy projectiles[1–5] and also with intermediate energy projectiles.[6] The product formation cross sections of nuclides with $A=70-170$ at a total incident projectile energy in excess of 1 GeV have been shown to be relatively energy independent.[3] The charge dispersions and the isotopic yield distribution curves for both neutron-deficient and neutron-rich products at various energies are nearly identical.[3] However, at intermediate projectile energies (^{12}C at 10–50 MeV/nucleon) the yields show strong dependence on the incident energy.[6,7] It has been suggested that more experimental data are needed to better understand the reaction mechanism at these projectile energies.[6]

The recoil properties of reaction products of high energy ^{12}C interactions with ^{238}U suggest that the process of formation of neutron-deficient nuclides is different from that of neutron-excessive products. The neutron-excessive products are formed via a low energy fission process, while the neutron-deficient products are believed to be formed mainly via spallation and high excitation fission processes.[3] Since the contribution from spallation can be assumed to be negligible at projectile energies near 20 MeV/nucleon, the neutron-deficient iodine isotopes can only come from fusion followed by fission or from nonequilibrium processes (fast fission,[8] etc.). These products can be distinguished from those arising from low excitation binary fission reactions by the fission fragment kinetic energies and the transfer of momentum inferred from recoil properties. The transfer of momentum to the fission fragments occurs most efficiently with intermediate energy projectiles.[9,10]

We have measured the yields and recoil properties of the products of the interaction of 20 MeV/nucleon ^{12}C with ^{238}U. In this paper, we report the iodine isotopic yield distribution and its interpretation with the liquid drop model. We also report the recoil parameters and use them to infer possible formation mechanisms.

II. EXPERIMENTAL

Three irradiations were performed, two of them followed by the radiochemical purification of iodine prior to gamma-ray counting. In the third experiment, only direct gamma-ray counting of the unseparated foils was performed. Cross sections were determined from the end-of-bombardment gamma-ray intensities.

A. Targets and irradiations

Each target stack consisted of a 27.4 mg/cm^2 natural uranium foil sandwiched between two pairs of 6.24 mg/cm^2 aluminum foils with 99.99% purity. The inner two aluminum foils (immediately adjacent to the target) served as forward and backward recoil catchers; the outer two served to protect the target stack against contamination by reaction products from the collimator and the beam stop.

Irradiations were performed with the 88-inch Cyclotron at the Lawrence Berkeley Laboratory. A 245 MeV $^{12}C^{5+}$ beam with an intensity of 20 electrical nanoamperes was delivered to the target foils. The 10-mm diameter of the beam spot was defined with an upstream collimator. The target foils were bolted to a copper block at the back of an electron-suppressed Faraday cup. The upstream aluminum foils degraded the energy of the beam incident on the uranium target foils to 240 MeV. The energy lost in the uranium itself was about 12 MeV.[11]

TABLE I. Decay properties and independent yields of measured iodine isotopes.

Isotope	Half-life	Principal γ ray (keV)	Abundance (%)	Independent yield (mb)
^{120}I	1.35 h	560	73.0	0.31±0.12
^{121}I	2.12 h	222	85.0	1.92±0.89
^{123}I	13.2 h	159	82.94	12.2±2.1
^{124}I	4.18 d	603	61.5	17.7±2.6
^{126}I	13.02 d	389	32.3	33.6±3.5
^{128}I	25.0 min	443	16.2	23.3±7.1
^{130}I	12.36 h	536	99.0	14.5±2.8
^{131}I	8.02 d	364	81.0	10.2±3.7
$^{132}I^{m+g}$	2.28 h	668	98.7	9.8±3.1
$^{132}I^{m}$	83 min	600	13.26	7.6±1.1
^{133}I	20.9 h	530	86.2	14.5±5.0
^{134}I	52.6 min	847	95.4	12.6±4.4
^{135}I	6.61 h	250	90.0	10.6±3.5

Irradiations were between 30 and 60 minutes in length. The deposited charge was recorded periodically throughout the bombardments to permit the reconstruction of the beam flux histories. Following each irradiation the foils were dismounted and rapidly transported to the chemistry laboratory or the counting facilities.

B. Chemical separations

In two of our experiments, the target and catcher foils were separately dissolved in aqua regia, in the presence of carriers, in a vessel equipped with an iodine vapor trap.[12] Several oxidation-reduction cycles were performed to ensure complete exchange between radioiodine and the added carrier. The iodine was extracted into CCl_4 and purified. In the final step, AgI was precipitated. The elapsed time between the end of bombardment and the final preparation of the precipitate for counting was 20 minutes. The chemical yields were determined gravimetrically. The samples contained no interfering contaminant activities.

C. Radioactivity measurements and data treatment

The gamma spectrometry was performed with four Ge(Li) detectors operated in conjunction with 4096-channel analyzers. The system was calibrated with a standard mixed radionuclide source. The energy resolutions, full width at half maximum (FWHM), of the detectors were between 2.0 and 2.3 keV for the 1332 keV gamma ray of ^{60}Co. The gamma-ray spectrum of each sample in the energy range between 50 keV and 2 MeV was measured at a pulse-height analyzer gain of about 0.5 keV/channel as a function of time for a total period of five weeks after the end of bombardment.

The gamma-ray spectra were analyzed with a set of computer programs, described in Ref. 13. These programs consist of a peak search, fitting, and integrating program (SAMPO), a sorting program for decay curve construction (TAU1), and an interactive decay curve identification program (TAU2). Since the accuracy of the initial activities determined with TAU2 is defined by the accuracy of the isotope table used in the identifications,[14] the intensity of each gamma ray was checked against more recent compilations[15,16] to improve the reliability of these data.

III. RESULTS

A. The independent yield

The end-of-bombardment activities were converted to cross sections, taking into account the chemical yield and the variation of the beam intensity during the irradiations. When several gamma rays were observed from the decay of the same nuclide, the cross section was calculated from the initial activity and abundance of each gamma ray, and the results were weighted and combined to give the final cross section and error bar for that nuclide.

Unfortunately, with the exception of yields for ^{124}I, ^{126}I, ^{128}I, and ^{130}I, the measured cross sections are cumulative. The program MASSY (Ref. 3) was used to calculate the independent yields. It was assumed that the yields for the isotopes of a given element were in the form of two overlapping Gaussians, and that the Gaussian parameters were slowly and regularly varying as a function of Z. The precursor distributions were estimated on the basis of 36 independent and cumulative yields from Sb ($Z=51$) to Nd ($Z=60$) with mass numbers between 112 and 146, determined from gamma-ray measurements of separated[17] and unseparated foils. Using the irradiation histories, the cross sections were iteratively corrected for decay during the bombardments and before the chemical separations. In Table I, the independent cross sections of the observed iodine nuclides are given, along with some of the decay data used in the calculations. The cross sections are plotted in Fig. 1.

The independent yields listed in Table I have not been corrected for contributions from secondary reactions. According to previous measurements,[3,12,18] the contribution to the formation of neutron-excessive iodine isotopes in a 27 mg/cm^2 uranium target foil is estimated to be about 3–10%. There is an increase of about 2% for each isotope from ^{131}I to ^{135}I.

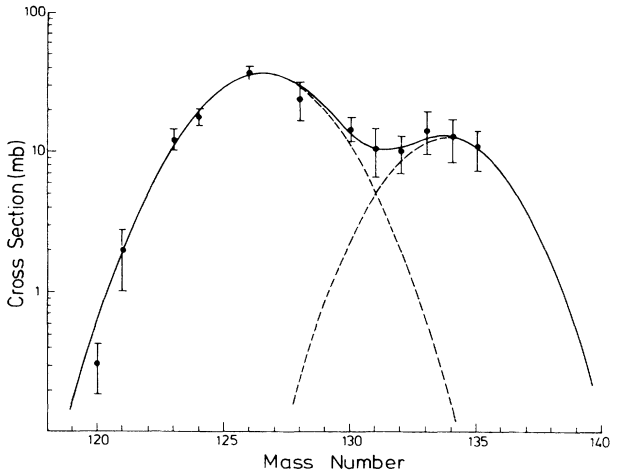

FIG. 1. The iodine independent yield distribution from the interaction of 20 MeV/nucleon ^{12}C with ^{238}U. The plotted points are the experimental values, and the solid line is the sum of the two fitted Gaussian distributions (dashed lines).

B. Recoil properties

The uncorrected gamma-ray activities at the end of bombardment measured in the forward and backward catcher foil samples and in the target samples were used in the range calculations. This assumes that any precursor nuclides have recoil properties similar to their iodine daughters.[2] The quantities determined in the recoil experiments are the fraction of the total activity of a given nuclide collected in the forward and backward catcher foils, denoted by F and B, respectively. The recoil properties of interest are the experimental range, $2W(F+B)$, and the forward-to-backward ratio, F/B. The target thickness is denoted by W. The correction for the effect of secondary reactions on recoil data is insignificant since the neutron-excessive products are produced from the normal binary fission process, which is nearly independent of the energy and identity of the incident particles. The values of the experimental range and F/B for the iodine nuclides are given in Table II and plotted in Figs. 2 and 3, respectively. The attached errors are due to the statistical uncertainties in the intensities of the gamma rays and the deviations between runs.

TABLE II. Recoil properties of measured iodine isotopes.

Isotope	F/B	$2W(F+B)$ mg/cm^2
^{121}I	1.69±0.27	7.76±0.72
^{123}I	1.80±0.25	8.01±1.06
^{124}I	1.82±0.28	7.91±0.67
^{126}I	1.86±0.28	7.51±0.66
^{130}I	1.62±0.23	7.70±1.03
^{131}I	1.23±0.20	7.73±1.04
$^{132}I^{m+g}$	1.10±0.25	8.00±1.20
^{133}I	1.04±0.15	7.34±1.12
^{134}I	1.08±0.11	7.75±0.45
^{135}I	1.03±0.18	7.10±0.62

IV. DISCUSSION

A. Parametrization of the isotope distribution

The 12 independent formation cross sections of iodine isotopes listed in Table I provide rather detailed information about the isotopic distribution. The occurrence of two maxima in the isotopic yield suggests a parametrization of the isotopic yield distribution in terms of two Gaussians. A nonlinear least-squares program was used to fit the measured cross sections with the expression

$$\sigma_I(A)=\sigma_{0D}\exp\left[-\frac{(A-A_{0D})^2}{2S_D^2}\right]+\sigma_{0E}\exp\left[-\frac{(A-A_{0E})^2}{2S_E^2}\right], \quad (1)$$

where the quantities indexed by E refer to the center of the neutron-excessive Gaussian and those indexed by D to the center of the neutron-deficient one.

The resulting isotopic yield distribution is shown in Fig. 1, and the Gaussian parameters are summarized in

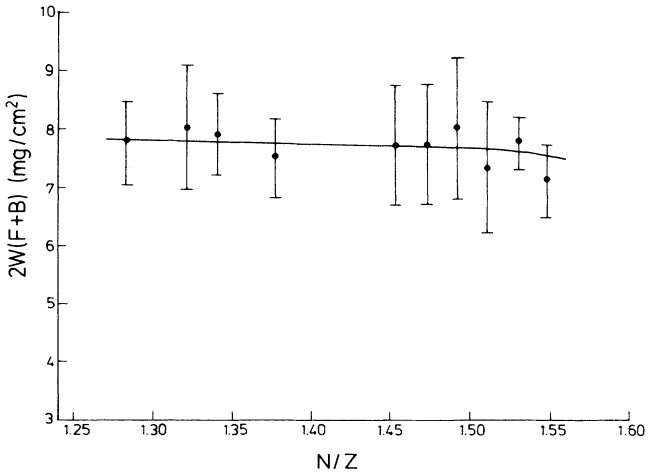

FIG. 2. Experimental range $2W(F+B)$ of iodine isotopes.

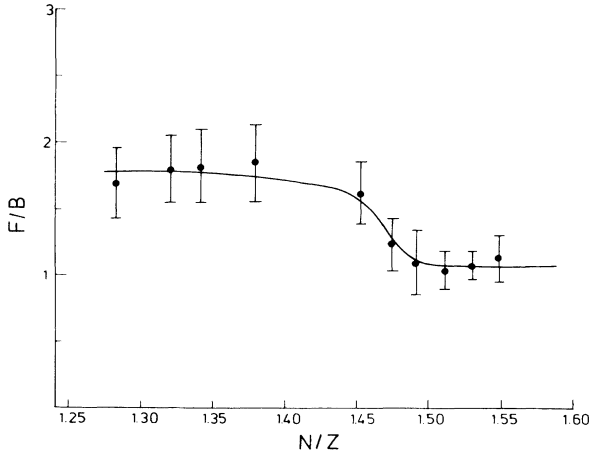

FIG. 3. Forward-to-backward ratios (F/B) of iodine isotopes.

TABLE III. Gaussian parameters of the iodine isotopic yield distribution.

	Neutron deficient	Neutron excessive
σ_0 (mb)	35.78±3.72	12.77±3.22
A_0 (mass unit)	126.52±0.34	133.78±0.71
S (mass unit)	2.29±0.22	2.04±0.24
σ_{tot} (mb)	205.4	65.3

Table III. The overall distribution is seen to consist of a rather low neutron-excessive yield and a much higher neutron-deficient yield. The neutron-excessive Gaussian peaks in the vicinity of ^{134}I and has a FWHM of 4.8 mass units; the area contributes approximately 32% of the total isotopic yield. It is reduced to approximately 30% when secondary effects are taken into account. The neutron-deficient Gaussian peaks midway between ^{126}I and ^{127}I and its FWHM is 5.4 mass units. The areas of both components of the iodine isotopic yield distribution (σ_{tot}) are given in Table III.

B. Comparison with isotopic distribution curves from other systems

To identify the formation mechanisms we have compared the iodine isotopic distribution curve (IDC) with the iodine IDC from the fission of ^{238}U by 40 MeV protons.[19] We normalized the σ_{max} of the p + U data by a factor of 0.56 and plotted it as the dashed curve in Fig. 4, along with the solid curve from this work. The yields from 40 MeV protons are distributed on a single Gaussian, with σ_{max} at $A=133.6$; the IDC overlaps the entire distribution of neutron-excessive iodine products from the ^{12}C-induced reaction. The FWHM of the neutron-excessive Gaussian from this work is 4.8±0.5 mass units, compared to 4.82 mass units from the 40 MeV proton-induced fission, which agrees within the experimental error. This information, together with the recoil properties (analyzed in subsections D and E), leads us to believe that the neutron-excessive iodine yields are formed by a low excitation energy binary fission process.

Next we compare the iodine IDC from our reaction with the cesium IDC produced in the reaction of 27 MeV/nucleon ^{12}C ions with ^{238}U.[6] For convenience of comparison we plot yield vs N/Z in Fig. 5. The solid curve represents the iodine yield from this work. The dashed curve represents the Cs yield from 27 MeV/nucleon ^{12}C + ^{238}U. We can see that the overall shapes of the distributions are similar. Both neutron-deficient yields peak at $N/Z=1.39$ and both neutron-excessive yields at $N/Z=1.52$, but the iodine IDC peak yields are higher than those of the Cs curve by a factor of about 1.8, though the widths of both components of the Cs curve are greater than those of the iodine IDC. The FWHM of the neutron-deficient component of the Cs IDC is 7.4 mass units, considerably larger than 5.4 mass unit width of the iodine curve. The FWHM of the neutron-excessive component of the cesium IDC is 6.0 mass units, also larger than the 4.8 mass unit width of the iodine curve. The total yield of iodine isotopes is 270 mb in this work, compared with the total yield of cesium of 150 mb in the 27 MeV/nucleon ^{12}C + ^{238}U reaction.

Finally, we compare the neutron-deficient yields of this work with the symmetric fission yields of mass $A=90-115$ from the reaction of 20 MeV/nucleon ^{12}C ions with ^{197}Au,[20] plotted as the dotted curve in Fig. 5. The symmetric fission yields from ^{197}Au have only a single peak at $N/Z=1.32$, compared with the peak of the neutron-deficient iodine yields from ^{238}U at $N/Z=1.39$. The difference in peak N/Z values reflects, in part, the difference in the N/Z values of the target nuclides. We expect very little contribution from the low excitation energy fission process with a ^{197}Au target; therefore, we can state that the neutron-deficient iodine yields are produced from a fission process other than the normal low excitation energy fission process, by a mechanism similar to that producing fission products in the reaction of 20 MeV/nucleon ^{12}C ions with ^{197}Au. This is possibly the

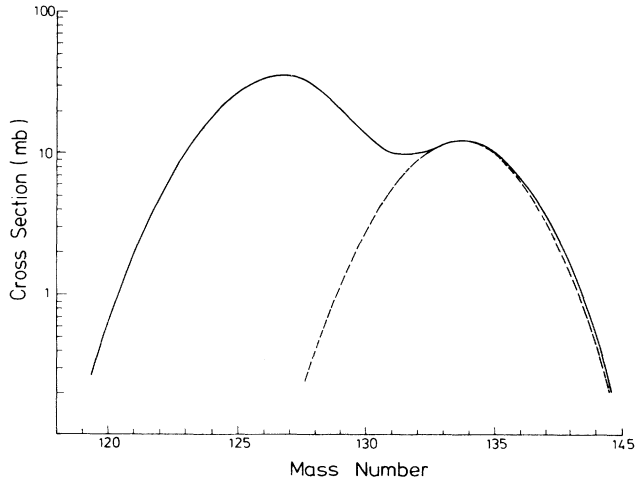

FIG. 4. Iodine isotopic distribution curve of this work (solid line) compared with that from the 40 MeV p + ^{238}U reaction (dashed curve).

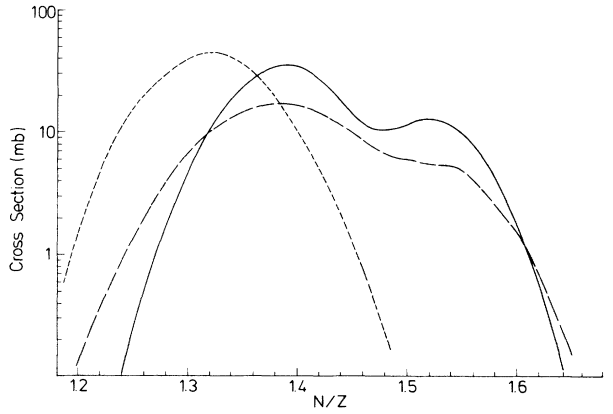

FIG. 5. Iodine isotopic distribution curve of this work (solid line) compared with the cesium isotopic distribution curve from the 27 MeV/nucleon ^{12}C + ^{238}U reaction (dashed curve) and the symmetric fission yields with mass numbers $A=95-115$ from the 20 MeV/nucleon ^{12}C + ^{197}Au reaction (dotted curve) on an N/Z plot.

fast fission process,[8,21] in which fissionlike fragments are produced from interactions at impact parameters producing composite angular momenta less than the critical angular momentum for fusion, yet greater than the value at which the fission barrier drops to zero due to centrifugal forces.

C. Theoretical analysis of the neutron-deficient yields

We have tried to understand the iodine yields arising from a fusion-fission process by minimizing the liquid drop model potential energy[22] to predict the most probable mass and the variance of the mass dispersion in the neutron-deficient isotopic distribution curve. The primary production of iodine fragments from ^{12}C on ^{238}U by fission competition in the deexcitation of the compound nucleus ^{250}Cf was computed with the help of the ALICE program. The most probable mass at $Z=53$ (iodine) is $A_p=135.5$. The most probable kinetic energy release in fission can be calculated from the semiempirical equation[23]

$$\bar{E}_{\rm kin}=0.1071Z^2/A^{1/3}+22.2 \text{ MeV} , \quad (2)$$

using the Z and A of the compound nucleus.

The average excitation energy of the iodine fragment, E_1^*, can be evaluated with the equation

$$E_1^*+E_2^*=E_{\rm c.m.}-\bar{E}_{\rm kin}+Q_0 , \quad (3)$$

where $E_{\rm c.m.}$ is the center-of-mass kinetic energy in the entrance channel, and Q_0 is the ground state Q value obtained from the entrance- and exit-channel mass excesses.[24] If we assume that the excitation energy divides among the fragments proportionally with their masses, the E_1^* of a primary fragment ^{135}I calculated in this manner is 135 MeV. This primary fragment deexcites mainly via the evaporation of neutrons. Using the modified DFF code,[3] we obtain a value of the most probable mass of deexcited iodine isotopes produced in the fusion-fission reaction of 125.6, in comparison with the experimental value, $A_{0D}=126.5\pm0.3$ (Table III).

If it is assumed that the neutron-deficient iodine isotopes arise via the fast fission process, we can calculate the expected variance of that portion of the iodine IDC, S_A. In the fissioning system, the charge variance at fixed mass asymmetry (scission) can be estimated[25] with the expression

$$S_Z^2=(1/C)\{\tfrac{1}{2}+1/[\exp(\hbar w/T)-1]\}\hbar w , \quad (4)$$

where C is the stiffness parameter arising from the minimization of the liquid drop potential energy of the fission of ^{250}Cf, w is the collective frequency, and T is the nuclear temperature. For fragments with $A=135.5$, a value of $C=3.36$ is obtained.[25] The temperature at scission is, approximately,

$$T=[(E_1^*+E_2^*)/a]^{1/2} , \quad (5)$$

where a is the level density parameter of ^{250}Cf. If $a=A/8$, then $T=2.83$ MeV. The collective phonon energy, $\hbar w$, has been estimated empirically[26] with the equation

$$\hbar w=(78 \text{ MeV})/(A_1^{1/3}+A_2^{1/3}) , \quad (6)$$

which gives $\hbar w=7.8$ MeV. The resulting value of $S_Z=1.15$ can be converted into the experimentally-observed mass variance S_A with the expression[25]

$$S_A^2=(A/Z)S_Z^2+S_E^2 , \quad (7)$$

where S_E is related to the width associated with neutron emission. The DFF code gives $S_E\simeq0.9$, resulting in $S_A=2.05$, in agreement with the experimental result of 2.29 ± 0.22.

TABLE IV. Comparison of the measured iodine isotope yield distribution parameters with theoretical predictions, assuming decay of a compound nucleus.

Parameters	Calculated	Experimental
S_Z	1.15	0.9±0.2[a]
S_A	2.05	2.29±0.22
A_0	125.6	126.5±0.34

[a]From the MASSY program.

The calculated parameters of the isotopic distribution, assuming a complete fusion intermediate, are compared with the experimental data in Table IV. The relative neutron richness of the experimental distribution and its marginally greater width imply that the neutron-deficient iodine yield comes from a nonequilibrium process, though substantial contribution from fusion-fission cannot be excluded on the basis of the IDC alone.

D. Recoil properties

The experimental range curve (Fig. 2) shows that the $2W(F+B)$ value of 7.8 ± 2.0 mg/cm^2 is obtained for all product iodine isotopes. With this range, the fragments have a kinetic energy of about 50–60 MeV. This can be understood as resulting from the binary fission process. However, the F/B curve (Fig. 3) shows a discontinuity. The neutron-deficient products have $F/B=1.8$, while the neutron-excessive products have $F/B=1.06$. Between these two flat curves there is an inflection point at ^{131}I. The process of formation of neutron-deficient products is different from that of the normal fission process. This is consistent with the isotopic distribution curve (Fig. 1).

E. Recoil parameters

The standard two-step velocity vector model developed by Sugarman and co-workers[9,27,28] has been used to transform the recoil data into kinematic quantities. In this model, the first step is the interaction of the incident particle (mass $M_{\rm HI}$, kinetic energy $E_{\rm HI}$) with the target nuclide to form a compound system (mass $M_{\rm CN}$, velocity $\bar{v}_{\parallel}$). The second step is the "fission" of this composite into two massive fragments. The velocity

TABLE V. Recoil parameters of iodine isotopes.

Isotope	R_0 (mg/cm^2)	$\eta_\parallel$	Kinetic energy (MeV)	$v_\parallel$ (MeV/nucleon)$^{1/2}$	E^* (MeV)
^{121}I	7.60±0.72	0.099±0.029	52.0±6.5	0.092±0.027	53±17
^{123}I	7.80±1.06	0.111±0.025	54.7±9.8	0.104±0.025	66±16
^{124}I	7.69±0.69	0.113±0.027	54.2±6.4	0.106±0.026	66±17
^{126}I	7.29±0.66	0.116±0.027	51.4±6.0	0.105±0.025	66±16
^{130}I	7.65±1.03	0.091±0.026	55.6±9.9	0.084±0.025	53±16
^{131}I	7.70±1.04	0.039±0.030	57.4±10.2	0.037±0.029	23±18
^{132}I	7.99±1.20	0.021±0.051	60.7±12.2	0.020±0.049	13±31
^{133}I	7.34±1.12	0.009±0.032	54.7±10.8	0.008±0.029	5±18
^{134}I	7.75±0.45	0.017±0.023	59.1±4.5	0.016±0.021	10±13
^{135}I	7.10±0.62	0.007±0.039	53.2±5.9	0.006±0.035	4±22

V of a fragment in the moving frame adds in vector fashion,

$$\bar{V}_L = \bar{V} + \bar{v}_\parallel \ , \tag{8}$$

where $\bar{V}_L$ is the measured fragment velocity in the laboratory frame, which can be evaluated from the mean range R by the relation

$$R = KV_L^N \ , \tag{9}$$

where N is a free parameter required by the Porile-Sugarman computer program, obtained from the slope of the plot of $\ln R_0$ vs $\ln V$ under the approximation

$$N = \partial \ln R / \partial \ln V \simeq \partial \ln R_0 / \partial \ln V \ , \tag{10}$$

where R_0 is the projection of the range along the initial vector $\bar{v}_\parallel$, obtained from the Northcliffe and Schilling range-energy table.[29]

The well-known Porile-Sugarman computer program, originally used for the fission of uranium with 450 MeV protons, may be modified for use with medium-energy heavy ions. The average deposition energy E^* will be

$$E^* = (0.8 E_{\rm HI} M_{\rm CN} v_\parallel) / [30.75 M_{\rm HI} (\gamma^2 - 1)^{1/2}] \ , \tag{11}$$

where the factor 0.8 is an empirical correction of the incident energy $E_{\rm HI}$ for prompt emission of a few nucleons,[27] and 30.75 is a factor necessary for the conversion of mass units into MeV. The relativistic factor γ can be expressed as follows:

$$\gamma = 1 + E_{\rm HI} / (0.9315 M_{\rm HI}) \tag{12}$$

for $E_{\rm HI}$ in GeV.

With these modifications, we are able to obtain derived recoil parameters from the measured recoil properties with the Porile-Sugarman program. The results of this analysis are summarized in Table V, and the average deposition energy E^* is plotted in Fig. 6. The quantity $\eta_\parallel = v_\parallel / V$.

The third column of Table V shows that kinetic energies are nearly constant among all observed iodine isotopes, with an average value of 55±10 MeV. However, the average deposition energy E^* and the forward momentum transfer $v_\parallel$ obtained for neutron-deficient iodine isotopes are higher than those obtained for the neutron-excessive isotopes by almost an order of magnitude. The value of E^* is about 60 MeV for the isotopes with $A \leq 130$ (as shown in Fig. 6), and drops to about 10 MeV for $A \geq 132$. The inflection point is also located at ^{131}I with $E^* \simeq 23$ MeV.

These results indicate that the neutron-excessive products were formed from a low excitation fission process, where very little kinetic energy was imparted to the center of mass of the fissioning system. The neutron-deficient products were formed from fission following a high momentum- and energy-transfer process; however, the expected value of $v_\parallel$ for a complete fusion reaction product is 0.30 MeV$^{1/2}$ nucleon$^{-1/2}$, a factor of 3 larger than our experimentally determined values. Therefore, the neutron-deficient yields arise predominantly from nonequilibrium processes in which full momentum transfer does not occur.

V. CONCLUSIONS

The measured yields of iodine isotopes, together with recoil ranges $2W(F+B)$ and F/B values obtained from the interaction of 20 MeV/nucleon ^{12}C ions with ^{238}U, provide a better understanding of the reaction mecha-

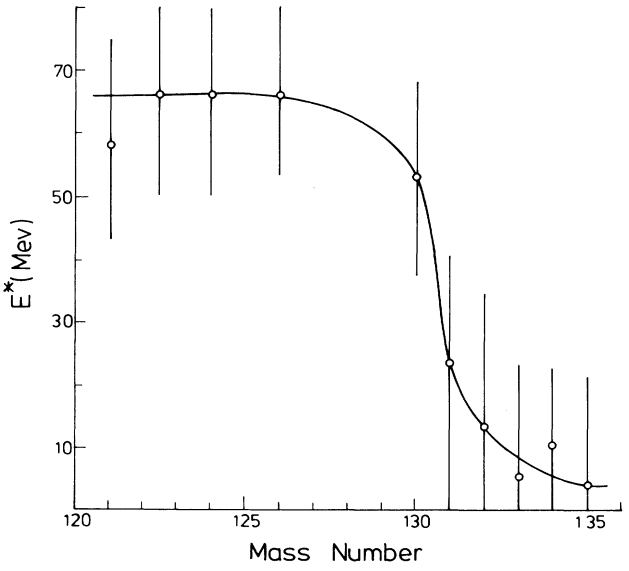

FIG. 6. Variation of deposition energy with mass number for iodine isotopes.

nism than does the determination of the yield alone. The results from the range data, consistent with the yield data, show that the mechanisms are dominated by two fission processes. The neutron-excessive products ^{132}I through ^{135}I are formed by a low excitation fission process. The target is excited through peripheral interactions, and fission follows the transfer of a few nucleons. Therefore the yield is quite similar to that formed from the low energy light-ion-induced fission process.

On the other hand, the neutron-deficient products ^{120}I through ^{130}I are formed from a high excitation fission process involving larger momentum and energy transfer, with smaller impact parameters and a large overlap of the incident carbon ions with the uranium target nuclide. These products arise primarily from a nonequilibrium process like fast fission or sequential fission, with little or no contribution from fusion-fission.

ACKNOWLEDGMENTS

The authors would like to thank the staff and crew of the 88-inch Cyclotron for their assistance and support. We would also like to thank K. Gregorich, R. Welch, and P. Wilmarth for their help. Two of us (Y.W.Y. and C.H.L.) wish to express our gratitude to the Lawrence Berkeley Laboratory for the hospitable stay, and one of us (C.H.L.) is grateful for the doctoral thesis research fellowship offered by the Ministry of Education of the Republic of China. This work was supported by the Division of Nuclear Physics of the Office of High Energy and Nuclear Physics of the U.S. Department of Energy under Contract No. DE-AC03-76SF00098.

*Present address: Lawrence Livermore National Laboratory L-232, P. O. Box 808, Livermore, CA 94550.

†Present address: Department of Chemistry, Faculty of Science, Niigata University, Niigata, Japan.

[1]W. Loveland, C. Luo, P. L. McGaughey, D. J. Morrissey, and G. T. Seaborg, Phys. Rev. C **24**, 464 (1981).

[2]Y. Morita, W. Loveland, P. L. McGaughey, and G. T. Seaborg, Phys. Rev. C **26**, 511 (1982).

[3]P. L. McGaughey, W. Loveland, D. J. Morrissey, K. Aleklett, and G. T. Seaborg, Phys. Rev. C **31**, 896 (1985).

[4]G. D. Cole and N. T. Porile, Phys. Rev. C **24**, 2038 (1981).

[5]N. T. Porile, G. D. Cole, and C. R. Rudy, Phys. Rev. C **19**, 2288 (1979).

[6]M. de Saint-Simon, S. Haan, G. Audi, A. Coc, M. Epherre, P. Gauimbal, A. C. Mueller, C. Thibault, F. Touchard, and M. Langevin, Phys. Rev. C **26**, 2447 (1982).

[7]M. de Saint Simon, R. J. Otto, and G. T. Seaborg, Phys. Rev. C **18**, 1651 (1978).

[8]Z. Zheng, B. Borderie, D. Gardes, H. Gauvin, F. Hanappe, J. Peter, M. F. Rivet, B. Tamain, and A. Zaric, Nucl. Phys. **A422**, 447 (1984).

[9]N. Sugarman, H. Munzel, J. A. Panontin, K. Wielgoz, M. V. Ramaiah, G. Lange, and E. Lopez-Menchero, Phys. Rev. **143**, 952 (1966).

[10]N. T. Porile, Phys. Rev. **185**, 1371 (1969).

[11]F. Hubert, A. Fleury, R. Bimbot, and D. Gardes, Ann. Phys. (Paris) **5**, 1 (1980).

[12]Y. W. Yu and N. T. Porile, Phys. Rev. C **7**, 1597 (1973).

[13]D. J. Morrissey, D. Lee, R. J. Otto, and G. T. Seaborg, Nucl. Instrum. Methods **158**, 499 (1979).

[14]I. Binder, R. Kraus, R. Klein, D. Lee, and M. M. Fowler, Lawrence Berkeley Report LBL-6515, UC-34C, 1977.

[15]*Table of Isotopes*, 7th ed., edited by C. M. Lederer and V. S. Shirley (Wiley, New York, 1978).

[16]U. Reus and W. Westmeier, At. Data Nucl. Data Tables **29**, 1 (1983).

[17]C. H. Lee, Y. W. Yu, D. Lee, H. Kudo, K. J. Moody, and G. T. Seaborg (unpublished).

[18]G. Friedlander, L. Friedman, B. Gordon, and L. Yaffe, Phys. Rev. **129**, 1809 (1963).

[19]M. Diksic, D. K. McMillan, and L. Yaffe, J. Inorg. Nucl. Chem. **36**, 7 (1974).

[20]H. Kudo, K. J. Moody, and G. T. Seaborg, Phys. Rev. C **30**, 1561 (1984).

[21]V. E. Viola, Jr. and T. Sikkeland, Phys. Rev. **130**, 1044 (1963).

[22]W. Reisdorf, M. de Saint-Simon, L. Remsberg, L. Lessard, C. Thibault, E. Roeckl, and R. Klapisch, Phys. Rev. C **14**, 2189 (1976).

[23]V. E. Viola, Jr., Nucl. Data **1**, 391 (1966).

[24]W. D. Myers, *Droplet Model of Atomic Nuclei* (IFI/Plenum, New York, 1977).

[25]H. Freiesleben and J. V. Kratz, Phys. Rep. **106**, 1 (1984).

[26]L. G. Moretto, J. Sventek, and G. Mantzouranis, Phys. Rev. Lett. **42**, 563 (1979).

[27]L. Winsberg, Phys. Rev. C **22**, 2116 (1980).

[28]J. J. Hogan and N. Sugarman, Phys. Rev. **182**, 1210 (1969).

[29]L. C. Northcliffe and R. F. Schilling, Nucl. Data Tables **A7**, 233 (1970).